Meso-Scale Finite Element Investigation into the Short and Long Term Strengths of Glass Fibre Reinforced Composites

Amar Khennane
khennane@usq.edu.au

Robert E. Melchers
rob.melchers@newcastle.edu.au

November, 2003

Faculty of Engineering & Surveying Technical Reports
ISSN 1446-1846

Report TR-2003-04
ISBN 1 877078 06 9

Faculty of Engineering & Surveying
University of Southern Queensland
Toowoomba Qld 4350 Australia
http://www.usq.edu.au/

Abstract

A finite element model is proposed for simulating the short and long term strength of Glass Fibre Reinforced Plastics. The essence of the model is a division of the composite system into a binary system comprising “fibre elements” to represent the fibres, and “effective medium” elements to represent the matrix material, which account for other mechanical properties such as shear and transverse stiffness and Poisson’s effect. Such a representation stems from the fact that the performance of a composite material is intrinsically controlled by the micro-structure of the component materials. Besides, it has the advantage of the power and versatility of the finite element technique. Typical results for short and long term strengths are compared to similar predictions obtained from shear lag theory. Good agreement is obtained for a variety of finite element discretisations.

TABLE OF CONTENTS

1 GENERAL INTRODUCTION

1.1 Preamble

Most of the world infrastructure, which was built just after the Second World War, is nearing the end of its life cycle. For the US only, the American Society of Civil Engineers (ASCE) estimates that the cost of bringing the infrastructure up to acceptable condition and functional performance levels will require nearly $1.3 trillion in investment over the next five years (CERF 2000-a). As a result, world wide, the leitmotiv seems to be on high-performance materials and systems. The high priority areas for this sector of the economy can be identified as (CERF 2000-b):
- reduction in project delivery time;
- reduction in operations/maintenance costs;
- increase in facility comfort and productivity;
- fewer illnesses and accidents;
- less waste and pollution;
- greater durability and flexibility.

For the construction industry, these goals must be accomplished within the framework of total life-cycle cost reduction.

Given their potential attributes such as: light weight, high stiffness-to-weight and strength-to-weight ratios, ease of installation in the field, potential lower systems level cost, and potentially high overall durability, composite materials are ideal candidates to fulfil these goals. The high performance attributes of FRP (Fibre Reinforced Plastics) have been realised by the civil engineering community and explains their rapid introduction. Indeed, this process has been so rapid in comparison to other civil engineering materials that the development of codes and guidelines, and the addressing of durability issues are seriously lagging behind.

One outcome of this rapid introduction is the lack of an “experience of use” basis, and therefore, the lack of easily accessible and comprehensive data on these materials, particularly data related to their capacity for sustained performance under harsh and changing environmental conditions. Most of the durability work on composites has focussed on aerospace and military applications. For these the operating life required is typically far shorter than that required of a bridge. Another factor that has contributed to the scarcity of data is the time required for long-term durability tests - they require a lot of time to carry out and are difficult to realise.

In summary, there is no doubt that for the new reinforced composites materials to gain widespread acceptance for use in the civil engineering infrastructure, the implications both for the short and long term strengths needs to be addressed.

1.2 Addressing the short and long term strength of GFRP

To address the long term strength of FRP materials for applications in infrastructure, it is important to identify the relevant issues. Unlike most other applications, for infrastructure applications structural components must be able to demonstrate satisfactory performance, with expected safe and serviceable life-times of fifty to one hundred years being typical requirements. In some applications they must do so at high stress levels, and often in aggressive environments. Since FRP composites are formed through the combination of micron-sized fibres in polymer matrices, the performance of the composite is intrinsically controlled by the micro-structure of the component materials, which in turn is controlled by the choice of constituent materials and the form, interface development and the processing

involved in manufacture. Minor changes in these matters can result in significant changes, not just in short-term performance, but also in the overall durability of the FRP composite. Factors such as bonding, void contact, and degree of cure and level of process-induced residual stresses are involved.

The matter of importance in durability behaviour is the different nature of the physico-chemical processes controlling long-term performance (Khennane and Melchers, 2000). Some of the processes may act together in synergy, thereby creating a combined mechanical and environmental degradation that could be more detrimental to the composite than the added effects of each one taken separately. This is a challenging issue since to predict the life of FRP structures with reasonable accuracy a precise and complete description of the processes that control the degradation of material properties (often lumped together under the generic name of "damage") is necessary. Unfortunately, such a picture does not exist at the present time.

Accelerated test methods and phenomenological modelling have been the predominant approach for establishing the long-term durability of FRP composites (CERF 1997). This consists of exposing specimens to environments harsher than they would encounter in service. The data is then used to extrapolate estimates of the likely long-term performance. However, as pointed out by Byars et al. (2001), accelerated exposure data and real time performance are unlikely to be closely related.

Evidently, the task of developing a viable life prediction model is complex and challenging. Of all the literature reviews (Schutte 1994, Chin 1996, Liao et al. 1998) addressing the issue, there is not one that did not stress the need for new studies and data concerned with long term performance and reliability in infrastructure applications.

As pointed out above, the performance of composite materials is controlled by the micro-structure. Understanding the degradation mechanisms taking place in the micro-structure under load is an important issue for structural design. In particular, it is useful to have a theory capable of assessing how details of the constituents and microstructure affect the resulting composite material behaviour. Therefore, instead of ignoring the lack of homogeneity, attention will be focussed on the internal structure of the material, as it is the latter that governs its behaviour and consequently its failure. The approach favoured therefore is the mesoscopic approach. It considers the damage progression in the constituents.

2 SHORT TERM UNIAXIAL STRENGTH OF GFRP

2.1 Introduction

Understanding the mechanisms of composite failure under load is important for structural design. In particular, it is useful to have a theory capable of assessing how details of the constituents and microstructure affect the resulting composite material behaviour. The approach developed here considers the damage progression in the constituents, the load transfer from broken fibres to the surroundings, as well as predictions of the ultimate strength.

Micro-mechanical models for strength of unidirectional fibre composite involve the modelling of the progression of fibre failure. The fibres are likely to have uncertain strength properties and these are commonly modelled as a random variable described by the so-called Poisson-Weibull probability distribution. This implies that the strengths between elemental (gauge–length) segments of fibre are statistically independent and that each elemental length has a strength described by the Weibull probability distribution. This idealisation is common in the modelling for fibre composites (Zhou and Curtin, 1995, Landis et al. 2000, Okabe et al.

2001). Details of the load re-distribution mechanism in the vicinity of single and multiple fibre breaks are required also. Different techniques for the load transfer from a broken fibre to the surrounding have been proposed in the past. Using the shear lag theory, the earliest study of the stress distribution around broken fibres in a three-dimensional unidirectional composite with aligned breaks was due to Hedgepeth and Van Dyke (1967). Sastry and Phoenix (1993) later improved this to include non-aligned breaks. More recent numerical based approaches have also been developed to analyse the tensile failure of unidirectional composites: the lattice Green functions model developed by Zhou and Curtin (1995), the shear lag model based on the finite element of Landis et al. (2000), and the 3-D shear lag approach developed by Okabe et al. (2001). However, all these models are restricted to being able to model only composite behaviour in tension. They precluded modelling of other damage mechanisms such as matrix cracking, fibre buckling and waviness. To address these shortcomings, the present paper employs the finite element method at the matrix/fibre scale as a first step in addressing these requirements for good quality modelling.

Although it was recognized that the finite element method can capture many of the key mechanical aspects, its use in the past at the matrix/fibre scale has been limited because of the extreme computational demand it required at such a scale (Reedy 1984). To date, only the six nearest neighbours around a fibre break have been analysed with finite element (Nedele and Wisnom, 1994). However, with recent progress in hardware technology, the high computational demands of the method can no longer be considered as the major hurdle regarding its application at this scale.

2.2 Finite element model of a unidirectional composite

The essence of the finite element model used in this study is a division of the composite system into a binary system comprising “fibre elements”, which represent axial tow properties only, and solid “effective medium” elements, which account for other mechanical properties such as shear and transverse stiffness and Poisson’s effect. This representation is derived from the bi-linear model developed by Cox et al. (1994) who used it to analyse 3D woven polymer composite systems for which the failure mechanisms depend very much on the architecture of the rovings. Figure 1-a shows a representative cell of a composite with the fibres arranged in a square array. To model this with the finite element method and to avoid discretising the fibres with 3-D elements, the binary model of Cox et al. (1994) is adapted to the matrix/fibre scale.

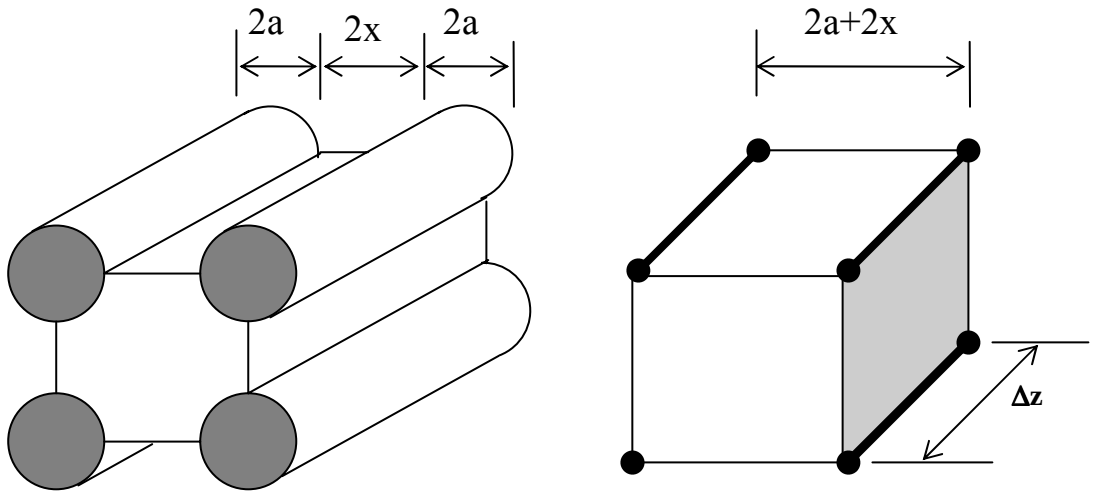

Figure 1-a: Finite element idealisation of a unidirectional composite

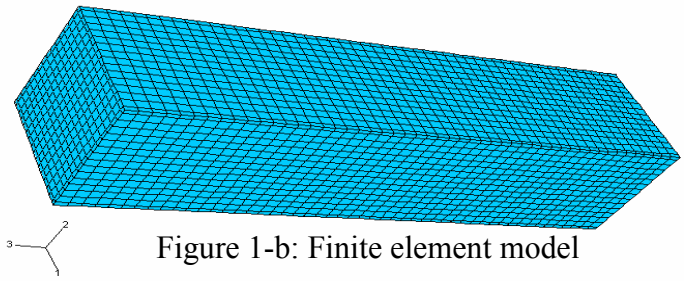

Figure 1-b: Finite element model

The tow elements accounting for axial properties are replaced by fibre elements, and the medium elements, which account for other properties, are replaced by matrix elements. Figure 1-b shows the complete finite element model. The fibre elements are two nodded line elements with no prescribed shear or bending resistance. The effective medium element can be considered homogeneous and isotropic. Both the effective medium elements and the fibre elements share the same coordinates in the initial undamaged state. As deformation and fibre damage occur, some relative displacements are likely to occur between them. This may be handled through the introduction of bond linkage elements. In practice, the stress strain relationship of the bond-slip elements can be obtained from a fibre pullout test. This particular aspect of bond slip is currently under investigation, herein no bond slip is tolerated between fibre and matrix.

For a volume fraction of fibre equal to ν, and a fibre diameter equal to 2a, such as shown on Figure 1-a, the dimensions of the cell, and therefore of the corresponding finite element, are given in Table 1.

Table 1: Dimensions of a representative finite element

Total area of square	$(2a+2x)^2$
Total area of fibre	πa^2
Fibre volume fraction ν	$\nu = \pi a^2 / (2a+2x)^2$
Value of x as a function of ν and a	$x = (a/2)(\Pi/ \nu)^{0.5} - a$
For a = 6.5 μm , ν= 0.542, x = 1.324μm	

In addition, the longitudinal length, Δz, of the element should be chosen carefully so that the element is not too short or too elongated when compared to the dimensions of the cell.

The number of finite elements required to model even a modest structural element is considerable and can make major demands on computer time. For example, a sample consisting of a square of 15 fibres and 1 mm long such as the one shown in Figure 1-b, requires a mesh of 16*16*50 = 12800 matrix elements, and 15*15*50 = 11250 fibre elements. As will be seen, a problem of this size can be handled relatively easily on a personal computer but much larger specimens undoubtedly will still require access to high power computing facilities. It follows that the level of discretisation necessary to capture the essential behaviour of a fibre composite is a matter of considerable interest.

2.3 Constitutive law for fibre and matrix elements

2.3.1 Reinforcing material

Throughout this paper the fibre elements are considered to have a linear elastic brittle behaviour. The Young's modulus of the elastic component, E_f, will be exactly equal to that of the reinforcing material; for example, for glass, $E_f = E_{glass}$. As a result, the axial stiffness of the fibre element is given by:

$$K_f = (E_f - E_m)A_f \quad (1)$$

where E_m is the elastic modulus of the matrix and A_f is the cross sectional area of the fibre. The substraction of E_m in defining K_f avoids double counting that would arise because the matrix elements fill all space.

2.3.2 Matrix material

In order to be able to compare the results of the present simulation with the results of the 3-D shear lag analysis of Okabe et al.(2001), three behaviour laws will be considered for the matrix: linear elastic, elasto-plastic, and elasto-plastic-brittle to represent cracking of the matrix.

For linear elastic behaviour the properties shown on Table 2 are adopted. These are the same as those used by Okabe et al. (2001).

Table 2. Material properties

Fibre Young's modulus	76 GPa
Fibre gage length L_0	24 mm
Fibre strength σ_0 based on L_0	1550 MPa
Fibre Weibull modulus ρ	6.34
Fibre volume fraction	0.542
Matrix Young's modulus	3.4 GPa
Matrix Poisson's ratio	0.35

The elastic-plastic behaviour will be assumed to be represented by the tensile stress strain curve shown in Figure 2 (Fiedler et al. 2001). To account for cracking of the matrix, it is assumed to lose its stiffness once the strain reaches 6 %.

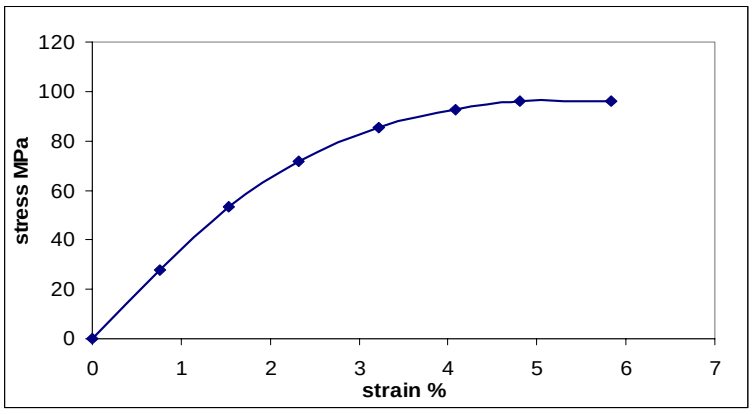

Figure 2: Representative tensile stress strain curve of a plain epoxy resin (Fiedler et al. 2001).

It should be pointed out that this stress strain curve was obtained for a plain epoxy resin, and the mechanical properties are similar to those used in (Okabe et al. 2001). Indeed, Okabe et al. (2001) used a matrix yield shear stress of 42 Mpa which is about half of the uniaxial yield strength shown in Figure 2. However the elastic moduli are nearly equal. In the present analysis, the effective plastic strains deduced from the curve in Figure 2 are introduced as tabulated values in the finite element analysis.

2.4 Computer simulations

Monotonic loading tests under deformation control were simulated. The simulation procedure was carried out according to the algorithm shown in Figure 3 and was implemented using the Abaqus® finite element package (Hibbitt, Karlsson & Sorensen, 2003).

Begin
Step 1: From a Weibull distribution assign each fibre element a strength σ_I
Step 2: Call Abaqus and run initial analysis
Step 3: Read FE results and evaluate stresses for all fibre elements.
Step 4: Failure of composite ? If YES, **STOP** the analysis, ELSE proceed to step 5
Step 5: Fail any element with a stress higher than its Weibull strength.
Step 6: Create a new input file for Abaqus to **remove** failed elements or to **increase** the imposed displacement
Step 7: Call Abaqus and **RESTART** the analysis with new input file
Step 8: Goto **Step 3**

Figure 3: Algorithm for the short term strength analysis

The algorithm is translated into a Python code. Python is a free object-oriented-scripting language (van Rossum G. 2001, Lutz & Ascher D. 1999). The Python script acts as a shell tool and calls Abaqus® finite element package whenever a finite element analysis is needed. This approach had to be used since the progressive failure of the fibres changes the finite element structure. Commercial finite element software does not appear to be able to solve such a problem directly. The reason for this is that user defined subroutines usually are written with reference to spatially defined (material) points. Thus, in the present case, all stresses acting on the elements need to be determined before they can be compared to the Weibull strengths associated with the elements. The comparison happens at model level not at material point level. Moreover, the fact that the strengths are random in nature makes it impossible to know à priori which element will fail first.

The analysis was carried as follows. Firstly, each fibre element was assigned a strength value from a Weibull probability distribution defined by:

$$\sigma_i^S = \left[Ln\left(\frac{1}{1-\eta_i}\right)\frac{L_0}{\Delta z}\right]^{\frac{1}{\rho}} \sigma_0 \qquad (2)$$

where η_i is a random number between 0 and 1 generated from a uniform distribution, L_0 is the fibre gage length, σ_0 is the fibre strength based on gauge length L_0, Δz is the length of fibre element, and ρ is the Weibull modulus for fibre strength. Next, an initial displacement was applied and the model was solved with the finite element package. The data base file generated by Abaqus for the analysis was then accessed and the stresses acting on the fibre elements were retrieved for comparison with the random fibre strengths. For any of the fibre

elements for which the applied stress was higher than its respective strength the element was removed with the Abaqus "remove element" option. The analysis was then restarted with the Abaqus "Restart option". If no element had failed, the prescribed displacement was increased and the analysis is restarted with the Abaqus "Restart option". This iterative process was carried out until a failure criterion was encountered.

2.5 Results

2.5.1 Stress strain curves

The above simulation procedure was applied to the finite element model shown in Figure 1. The material properties used are shown in Table 2 and are similar to those used in the shear lag model of Okabe et al. (2001).

As noted, the sensitivity of the solution to discretisation is of interest. In order to assess this, the effects of specimen size (number of fibres) and longitudinal length (Δz), were analysed for six different models:

i. 10 by 10 fibres and 100 longitudinal elements (Δz = 10 μm) which corresponds to a length of 1 mm;
ii. 10 by 10 fibres and 50 longitudinal elements (Δz = 20 μm) which corresponds to a length of 1 mm;
iii. 15 by 15 fibres and 100 longitudinal elements (Δz = 10 μm) which corresponds to a length of 1 mm;
iv. 15 by 15 fibres and 50 longitudinal elements (Δz = 20 μm) which corresponds to a length of 1 mm;
v. 20 by 20 fibres and 100 longitudinal elements (Δz = 10 μm) which corresponds to a length of 1 mm,
vi. 20 by 20 fibres and 50 longitudinal elements (Δz = 20 μm) which corresponds to a length of 1 mm.

Furthermore, so as to assess the effect of randomness on the solution, the analysis was repeated 30 times for each model using a different random sequence for fibre strength. The obtained stress strain curves were compared to each other and also compared to the results of Okabe et al. (2001). These authors used 20 by 20 fibres and 100 elements (Δz = 10 μm) along the longitudinal direction.

Figure 4 shows the stress-strain curves obtained as means of thirty elasto-plastic simulations for each of the six different models. The curves have the same shape as that obtained with shear lag theory (Okabe et al. 2001). The predicted ultimate stresses and stiffness are slightly higher than those predicted with shear lag theory. This is to be expected since in shear lag theory, the strength and stiffness contribution of the matrix are neglected. Figure 4 also shows the contribution of the matrix. It can be seen that the matrix does carry some normal stresses although these are very small compared to those carried by the fibres; being negligible in the early stages of loading and then increasing to 3 % at peak stress. Figure 4 also shows that the number of fibres and the element length do not have any obvious effect on the results, both for ultimate strength and for stiffness. The little difference, which there is between the curves, is considered to be due mainly to the randomness in fibre strengths. As it appears, this result suggests that the number of fibres and the degree of finite element discretisation of the specimen do not affect the results obtained for the shape of the stress-strain curve or for the ultimate strength of the composite specimen. The truth is that the specimens are still very much similar in size to induce any size effect in the curves. Figure 5 from Okabe and Takeda (2002) shows size effect on the bundle strength of CFRP. It can be clearly seen that there is no significant difference between the strength of bundles that are

2×10^5 fibres apart. Or, in this proper case, the difference in the number of fibres between the models is even much smaller. Furthermore, with currently available hardware, it is impractical to carry any finite element simulations to display any size effect, given the sheer sizes of the models required.

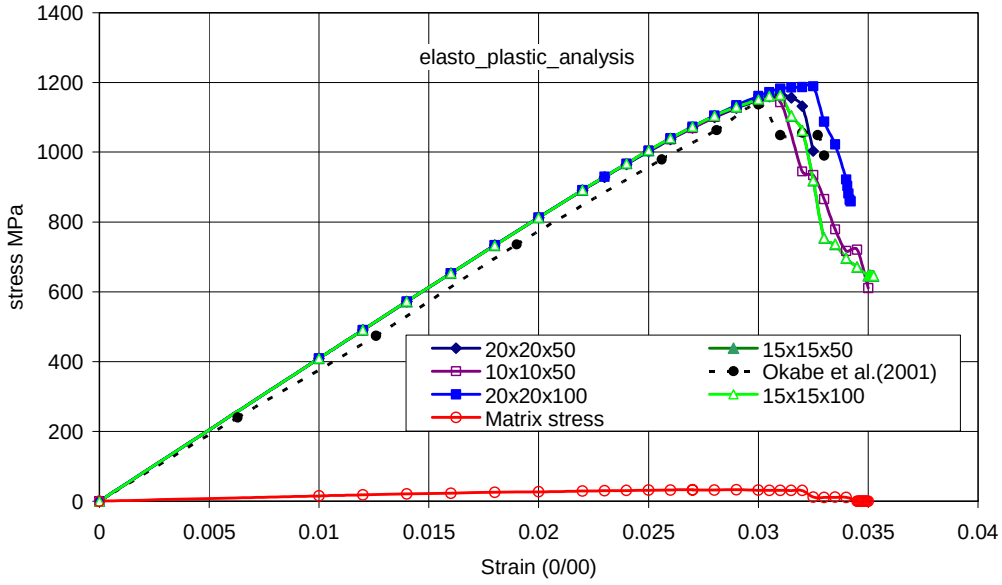

Figure 4: Computed stress strain curves for various finite element discretisations and element sizes

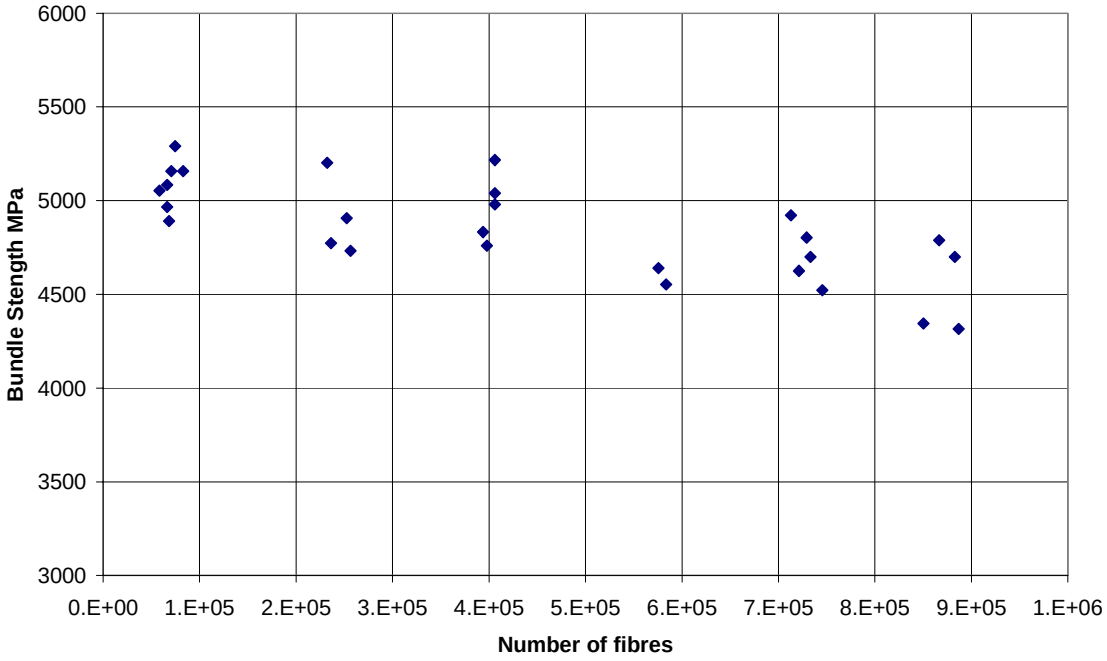

Figure 5: Size effect in bundle strength from Okabe and Takeda (2002)

2.5.2 Effect of matrix cracking

Matrix cracking in tension is accounted for in the model through a damage parameter (Chang and Lessard, 1991). The matrix is assumed to lose its strength and stiffness once the strain reaches 6 %. The results are shown on Figure 6. As it appears, cracking of the matrix

has no effect neither on the stiffness nor on the strength. This is no surprising since as shown on Figure 4, the matrix carries little or no stress compared to the fibres.

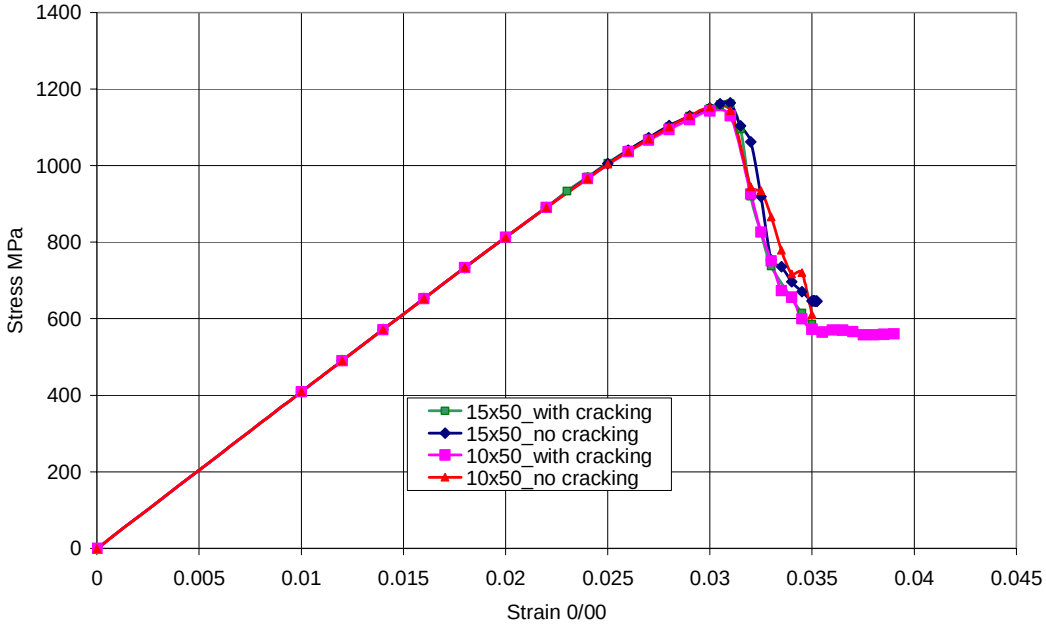

Figure 6: Effect of matrix cracking

2.5.3 Stress concentration factors in fibres and resin

The stress concentrations in the vicinity of a broken fibre element are of interest in design. The following figures illustrate stress concentration effects. The calculations were based on Figure 7, which shows the fibre for which the stresses were calculated.

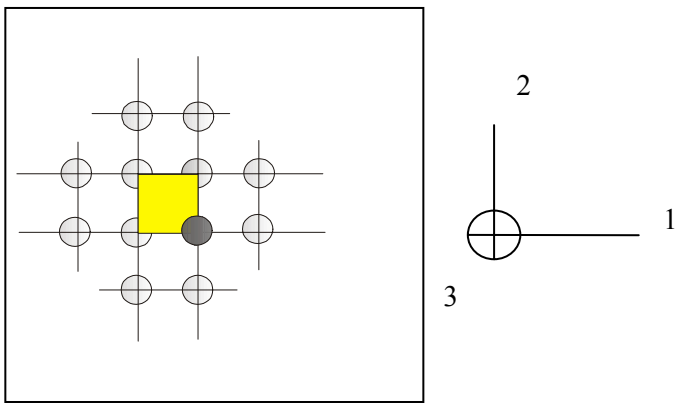

Figure 7: Relative position in cross section of matrix and fibre elements

Figure 8 shows the longitudinal stress in the fibre as a function of applied strain for the 10 by 10 fibres and 50 longitudinal elements model. At a strain of 0.026, the fibre is still intact. However, at strain of 0.027 the fibre breaks at 11^{th} element along the longitudinal direction. As a result the longitudinal stress has dropped to zero at the broken element position. It takes about 10 elements from each side of the break for the stresses to recover to their original levels. This yields a stress recovery length equal to 0.40 mm, which is in agreement with the value of 0.42 mm obtained by Okabe et al. (2001) with shear lag theory. As the loading is increased, the stresses in the fibre increase also but not in a uniform manner. This lack of uniformity is obviously caused by stresses transferred from breaks in neighbouring fibres. At a strain of 0.032, another break happens in the fibre at element 40. It

can be clearly seen on the graph that this is the result of a stress concentration being developed at the location due to breaks in the neighbouring fibres.

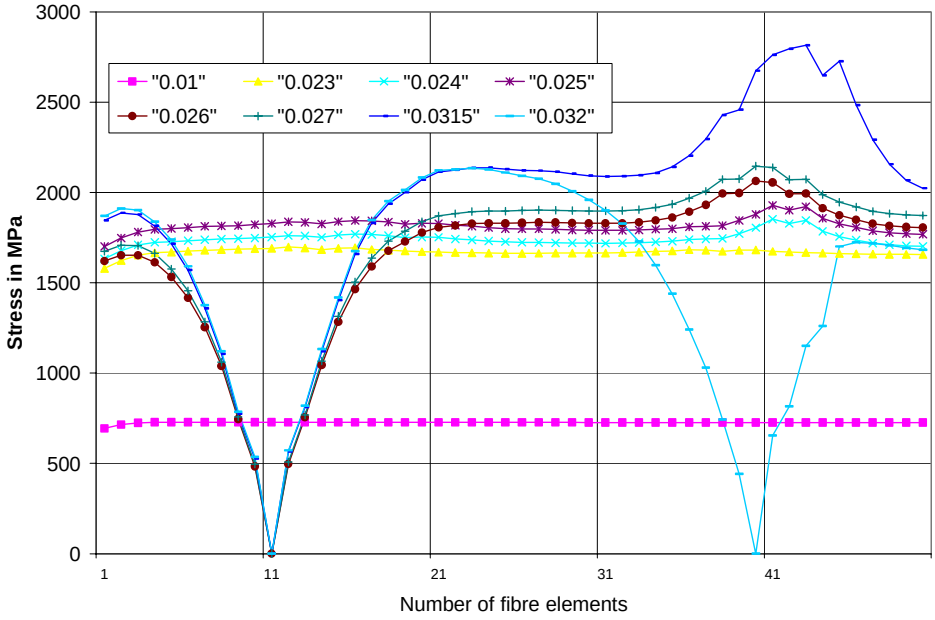

Figure 8: Longitudinal stress in fibre as a function of applied strain (elasto-plastic analysis)

Figure 9 shows the longitudinal stress in the fibre as a function of applied strain for the 15 by 15 fibres and 100 longitudinal elements model including cracking of the matrix.

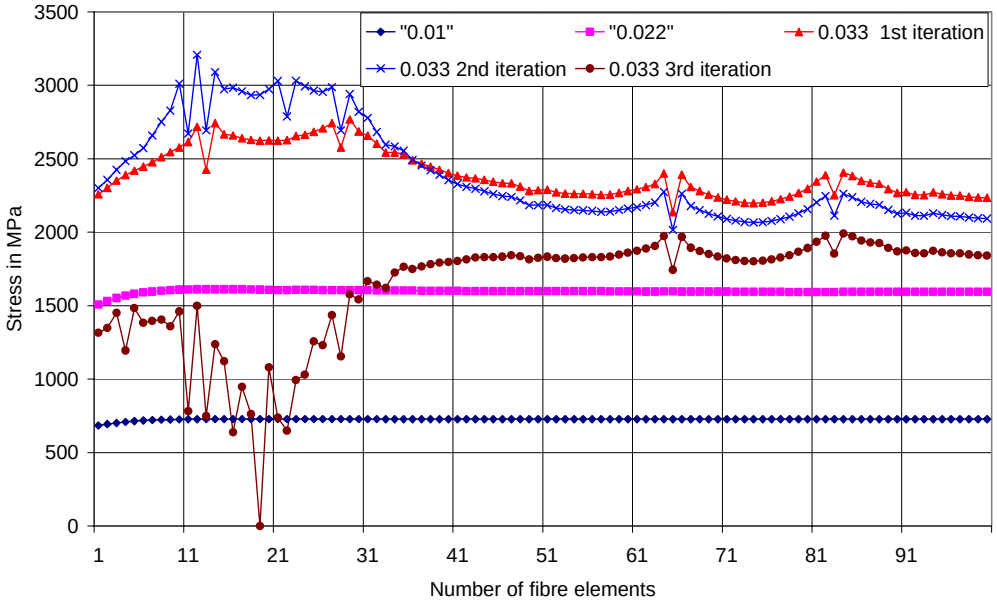

Figure 9: Longitudinal stress in fibre as a function of applied strain (elasto-plastic with matrix cracking)

At a strain of 0.022, the stress distribution in the fibre is uniform. However, at strain of 0.033, a build up of a stress concentration is noticeable in the neighbourhood of element 20. At this strain value, some fibres break somewhere, and the model performs an iteration to restore equilibrium. As a result, the stresses from the broken fibres are redistributed, causing a pronounced increase in the stress concentration around element 20, which leads to its failure at the third iteration. The failure of element 20 is accompanied by matrix cracking in its vicinity, creating a disturbance zone of which extends over about 10 elements on each side of

the break. This disturbance zone corresponds to a distance of about 0.2 mm and is noticeable by the "saw tooth" shaped stress curve. This suggests that when a fibre breaks a high proportion of its load is redistributed to the neighbouring matrix leading to more damage. The stress in the fibre takes about 19 elements from each side of the break to recover to its original levels. This yields a stress recovery length equal to 0.38 mm, which is in agreement with the value obtained above.

2.6 Discussion

The finite element model is used in conjunction with the Weibull fibre strength probability law to model the short term uniaxial strength of GFRP. The problem of stress redistribution around broken fibres in composite was presented. The method adopted allowed, with little approximation other than that inherent in finite element modelling, the progression of fibre failure to be modelled and followed. As far as can be ascertained, this is the first time that the finite element method has been used in such an extensive manner and at such a scale. Previously, only the six nearest neighbours around a single fibre break have been analysed with FEA. The model revealed that the matrix carries little or no stress when compared to the fibres. It was also found that when a fibre breaks a high proportion of its load is redistributed as normal stresses to the surrounding matrix creating a disturbance zone which extends over a distance of about 0.2 mm. While it would have been useful and interesting to be able to compare the results with actual experimental observations, these do not appear to exist at the required level of detail. What has been possible is a comparison with results predicted by shear lag theory. In general the results developed here compare well with those predicted by shear lag theory. The latter have been replicated quite accurately

3 LONG TERM STRENGTH

3.1 Introduction

Moisture induced stress-strain corrosion is increasingly being seen as a critical issue for the long term strength of glass reinforced plastics composites. However, except for the works of Wierderhorn and Bolz (1970) on bulk glass and those of Sekine et al. (1998) for and Khennane and Melchers (2003) for GFRP, there is little published work on the development of fundamentals laws, which permit the valid extrapolation of stress rupture curves to long service lives. As a result, design guidelines for GFRP components have been developed mainly on a prescriptive rather than on a performance basis. Roberts (1978), cited in (Lyons and Phillips 1981) described three bases used to determine the design stress for such components. The first consists of using the tensile strength obtained from a short-term test, and then dividing it by a "factor of safety", usually in the range eight to sixteen. The second approach is to specify a permissible design strain and to multiply it by the short-term modulus of elasticity. As a third approach, long-term stress-rupture tests could be performed, and the design stress could be chosen from a given lifetime. The stress levels so obtained would be reduced by a further factor of safety, again arbitrary, to allow for the detrimental effects of the environment.

Given the fact that the use of composites in the infrastructure industry is relatively recent, and that there is a lack of an "experience of use" basis, the development of performance criteria demonstrating compliance with such criteria is an apparent need. To meet this need, and therefore to contribute to the wider acceptance of composites by the

infrastructure industry, it is considered that analytical methods that help explain and understand the mechanisms and rates of environmental degradations for GFRP are required.

3.2 Environmental stress corrosion in GFRP

The stress corrosion of bulk glass involves both ion exchange and silica network destruction (Charles 1958a,b). According to Charles (1958a,b) who postulated a corrosion mechanism for glass, the first step in the reaction is an ion exchange between the Na end of the glass network and hydrogen ions from the water, which is then followed by base hydrolysis of the silica network:

$$\left[\begin{array}{c} ! \\ -Si-O-Na \\ ! \end{array} \right] + H_2O \rightarrow - \underset{!}{\overset{!}{Si}} OH + Na^+ + OH^- \qquad \text{(i)}$$

$$\left[\begin{array}{ccc} ! & & ! \\ -Si-O- & & Si- \\ ! & & ! \end{array} \right] + OH^- \rightarrow - \begin{array}{c} ! \\ Si-O-H \\ ! \end{array} + - \begin{array}{c} ! \\ Si\,O^- \\ ! \end{array} \qquad \text{(ii)}$$

$$\left[- \underset{!}{\overset{!}{Si}} O^- \right] + H_2O \rightarrow - \underset{!}{\overset{!}{Si}} OH + OH^- \qquad \text{(iii)}$$

This reaction is autocatalytic, and the result is flaw formation at the surface. As established by Mould (1960) and Wierderhorn and Bolz (1970), these surface flaws concentrate applied stresses to critical values that ultimately cause the failure of the glass.

As in bulk glass, the premise for stress corrosion in glass fibres is that a stress corrosion crack initiates at a pre-existing flaw in a glass fibre. The crack then grows under stress and finally leads to breakage of the fibre. However, in GFRP this can happen only after aggressive environment components have diffused through the resin protecting the glass fibres. This is the phenomenon of environmental stress corrosion and for glass fibres, including those embedded in a polymer matrix, has been studied by many researchers. An excellent review of the subject is given in (Schutte 1994). For aqueous environments more details are given in (Schmitz and Metcalfe 1966, Lyons and Phillips 1981, Phillips 1983, Hogg and Hull 1982).

3.3 Role of flaws and their characterisation

From the above description, it is evident that stress corrosion failure of GFRP is closely linked to the flaws in the fibres. These flaws act as stress risers. The matrix material serves mainly to transfer the load between the fibres. The two factors controlling fibre failure are (i) the statistical distribution of fibre flaws, and (ii) the stress distribution along the fibre direction.

According to Schmitz et al. (1965) flaws in glass fibres are extremely small. Conventional methods of examination are difficult to use and even if successful, the results do not readily describe the effect of the flaws on strength. As a result an indirect method has been used to characterise the flaws. It consists of a logarithmic plot of fibre strength versus sample length. Typically the plot is linear, but only for limited ranges of gages lengths (lengths of the fibre sample tested). The explanation, which has been offered for such a result is that two distributions of flaws are present on the fibres. One distribution of flaws controls failure for long lengths (type A) and the other one (type B) controls failure for short lengths. Type A flaws are 2 cm apart on the average and are believed to be deep pits or scratches.

Type B flaws have an average separation of 10^{-2} cm or less and are believed to be shallow etch pits formed by water vapour attack.

Combining the technique of UV light absorption and hydrofluoric acid etching, Bartenev (1969) also characterised the different types of flaws in a glass fibre. According to his representation, shown in Fig. 10, three levels of strength σ_0, σ_1, σ_2 correspond to three different types of flaws present on the surface of a glass fibre. The level of strength σ_0 was found to result from heat treatment, which leads to micro-cracks having a depth comparable to half the radius. The strength level σ_1 corresponds to surface submicro-cracks generated during the drawing of the fibre. In general, their depth is less than the surface layer of 0.01 μm. Strength level σ_2, corresponds to the existence of microruptures on the surface of the fibre, these also occur during drawing. The stress level σ_3 corresponds to the strength of flaw-less glass. Even though the description given in (Bartenev 1969) is more precise in terms of size and shapes of the individual flaws, it does not consider the distribution of the different flaws over the fibre length. Comparing the two flaw characterisations just described, it is possible that type A and Type B flaws of Schmitz et al. (1965) correspond respectively to the σ_1, σ_2 flaws of Bartenev (1969). Using the descriptions given above, the following section attempts to demonstrate that this equivalence is likely.

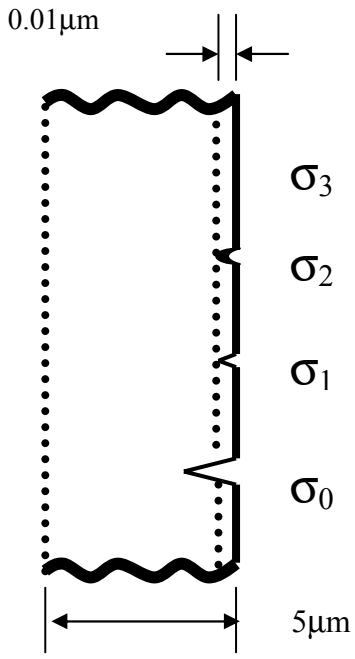

Figure 10: Schematic representation of flaws on the surface of a glass fibre (Bartenev1969)

3.4 Modelling of stress corrosion cracking of a glass fibre

3.4.1 Sekine et al. [1998] model for stress corrosion cracking of a glass fibre

Based on the equation for the rate of stress corrosion of bulk glass in water (Wierderhorn and Bolz 1970), given as:

$$\frac{da}{dt} = \nu \exp\left(-\frac{E_a - \alpha K_I}{RT}\right) \tag{3}$$

where a is the length of the crack, E_a is the activation energy, K_I is the stress intensity factor for opening mode, R is the gas constant, T is the absolute temperature and ν and α are empirical constants.

By assuming that the shape of a flaw in a fibre is circular, as represented in Fig. 11 from Sekine et al.(1998), equation (3) can be rewritten in the form of the rate of increase of the half angle θ with time as:

$$\frac{d\theta}{dt} = \frac{C_W}{2r\sin\theta}\exp\left(\frac{\alpha K_I}{RT}\right) \tag{4}$$

with $C_W = \nu \exp\left(\frac{\alpha K_I}{RT}\right)$ (5)

By further assuming that the stress intensity factor K_I can be approximated as:

$$K_I = \sigma\sqrt{1 - \cos(\theta)}\sqrt{2\Pi r} \tag{6}$$

equation (4) was integrated between θ_0 (initial angle) and θ_F (final angle) to obtain the time t_F it takes to a fibre to rupture by stress corrosion:

$$t_F = \frac{4rRT}{C_w\,\alpha\sigma\sqrt{\Pi r}}\left(\frac{RT}{2\alpha\sigma\sqrt{\Pi r}} + \frac{\theta_0}{2}\right)e^{-\frac{\alpha\sigma\sqrt{\Pi r}}{RT}\theta_0} \tag{7}$$

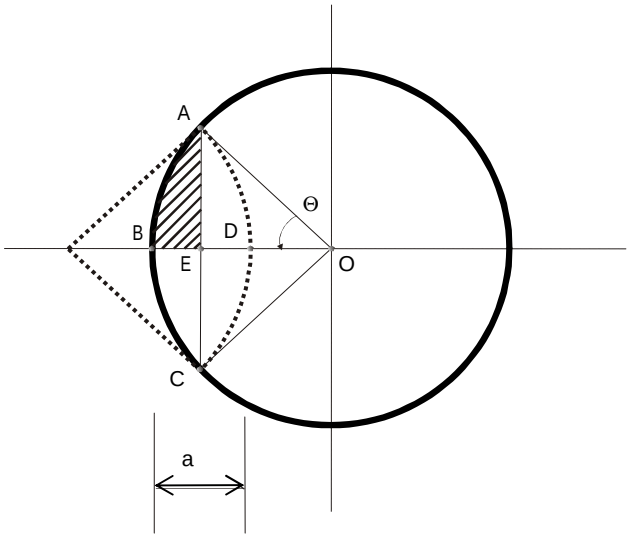

Figure 11: Shape of a stress corrosion crack in a crack fibre (Sekine and Beaumont 1998)

Once the time t_F was found, Sekine et al. (1998) extended the fibre model to approximate the stress corrosion of a laminate. By assuming that the time required to the brittle fracture of a glass fibre and surrounding matrix is much shorter that t_F, they went on to estimate the macroscopic propagation rate in the laminate as being the ratio of the distance between two rows of fibres divided by the time t_F. The distance between two fibres takes

different values depending on the disposition of the fibres. However, this approach is not consistent with the random nature of fibre flaws. If such an approach is used, there is the difficulty of choosing the localisation of the initiation of the crack. Or in a composite structure, a stress corrosion crack is likely to initiate at the weakest point; that is the point where the fibre with the biggest flaw is localised, which is completely random in nature.

3.4.2 Calibration of the Sekine et al fibre model

When the values of the parameters ν, E_a, α (for water), the values θ_0, r, T, and σ are set, the rupture life of an E-glass fibre can be predicted in an aqueous environment using equation (7). The data given in (Wiederhorn and Bolz 1970) obtained for an aluminosilicate glass tested in water at 25 ^{o}C are adopted since the composition of this glass is very close to that of E-glass. The values of the different parameters are shown on Table 2.

Table 2: Data for rupture life predictions of E-glass in two different environments

Aqueous environment
$E = 1.212\ 10^{5}$ J/mol
$\ln\nu = 5.5 \Rightarrow \nu = 244.7$
$Cw = 9.763\ 10^{-20}$
$\alpha = 0.138$
$r = 5.\ 10^{-6}$ m
$T = 296\ ^{o}K$
$R = 8.31$ J/mol/^{o}K

The results of numerical simulations carried out with the above data are shown in Figure 12. The stress levels considered range from 0.3 GPa to 3.3 GPa. Since, as discussed previously, the shapes and sizes of the flaws are not exactly known, different values of the initial angle θ_0 were used. It can be seen that each value of θ_0 gives a different curve.

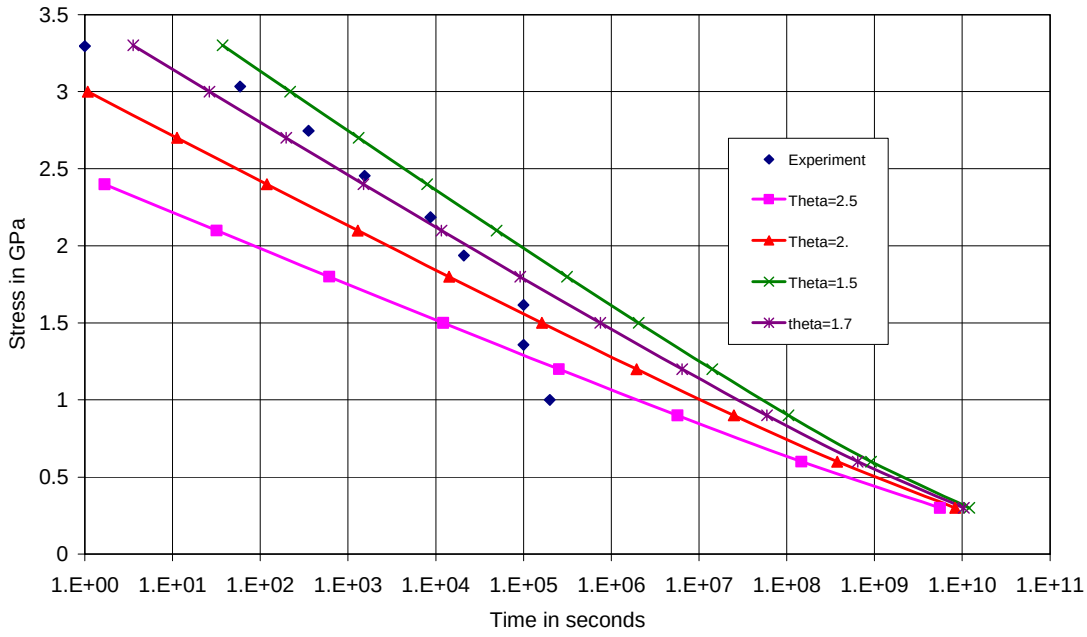

Figure 12: Stress corrosion of a glass fibre in 100 % RH

The experimental results of Schmitz et al.(1966) are shown also, it can be seen that the value of $\theta_0 = 1.7^o$ corresponds most clearly with the experimental results. In contrast, the value $\theta_0 = 2.5^o$ used by Sekine et al. (1998) in their simulation work, and which corresponds to a flaw with a depth of 0.01 μm, does not lead to a particularly good agreement with the experimental results. It underestimates the life of the fibres. Considering that the results reported in (Schmitz and Metcalfe 1966) were obtained for a fibre gage length of 2.54 cm (1 inch), this suggests that flaw A, which has a lower probability of occurrence over the same gage length than flaw B, corresponds indeed to flaw σ_1 having a typical depth of 0.01μm.

3.5 Stress corrosion of GFRP

3.5.1 General

The previous section has shown how the Sekine et al. (1998) model for the stress corrosion failure of a glass fibre can be calibrated against limited experimental results. The present section deals with the stress corrosion of a bundle of fibres embedded in a matrix material. The fibres are assumed to be straight and in tension. However, instead of trying to approximate the macroscopic rate of a stress corrosion crack, which is not consistent with the random nature of fibre flaws, the life of the bundle is obtained here as a sum of the lives of the individual fibres. This is a complex phenomenon as it depends on the probability of fibre fracture and the sequencing of fibre fracture. Numerical simulation of this phenomenon seems to be an appropriate solution strategy. The stress distribution from a broken fibre to the neighbouring unbroken fibres and the matrix is achieved herewith using the previously developed finite element model. The fibres are assumed to behave in a linear elastic manner. The polymer matrix is assumed to behave according to an elastic-plastic law as represented on Figure 2.

3.5.2 Simulation procedure

The time-to-failure is computed according to a scheme similar to that developed by McBagonluri (1998). Figure 13 shows the algorithm of the simulation procedure. The simulation procedure was implemented within a Python script calling the Abaqus® finite element package (Hibbitt, Karlsson & Sorensen, 2003) to carry out the load redistribution from a broken fibre to the neighbouring matrix and undroken fibres.

Begin

Step 1: From a normal distribution assign each fibre element a half angle θ generated from an appropriate statistical distribution of flaw size.

Step 2: Time = 0

Step 3: Call Abaqus and carry out Finite element analysis

Step 4: Read FE results and evaluate stresses for all fibre elements.

Step 5: Using equation (7), find the smallest time (Δt) that will give the next fibre break.
Time = Time + Δt

Step 6: Has the composite failed?
If **NO,** Update the half angle θ for all the non failed fibre elements due to corrosion that occurred during Δt, and create a new input file for Abaqus to **remove** failed element.
GOTO STEP 3
If **Yes** Life=time
End

Figure 13: Algorithm for the long term strength analysis

In the present case, each fibre element is assigned a half angle θ generated from an appropriate statistical distribution of flaw size. To avoid edge effect, the edge elements are assigned the smallest half angle θ. This ensures that they will be the last elements to fail. Once this is done, a finite element analysis of the model is carried out to obtain the stresses acting in the elements. Using equation (5) the failure time is estimated for each element. The smallest time, Δt, is chosen as the one that will give the next fibre break. A check is then made as to whether the composite has failed or not. If the composite has failed, the process is stopped and its life recorded as the sum of the individual time elements $t_f = \Sigma\Delta t_i$. If the composite has not failed, the half angle θ must be updated for all the non-broken elements and since stress corrosion will have occurred during the time Δt,. Since there is no expression that gives the angle θ at the end of an elapsed period of time t_f , this has to be updated by integrating numerically equation (4). The above process repeated until failure occurs. The composite is considered as having failed or reached its life cycle once the increment in time Δt is very small; ie the curve failure events versus time reaches a stationary plateau.

3.5.3 Numerical integration of equation 4

Equation (7) is very useful in estimating the life of a glass fibre. However, it does not give any indication on the final value θ_f of the half angle. Actually it is independent of θ_f. When it comes to estimating the increase in the crack size at the end of an arbitrary elapsed time period, such as

$$\int_{\theta_0}^{\theta_t} d\theta = \int_{t_0}^{t} \frac{C_w}{2r \sin\theta} \exp\left(\frac{\alpha K_I}{RT}\right) dt = \int_{t_0}^{t} F(\theta)\, dt \tag{8}$$

equation (7) is of no use. To obtain this increase, it becomes necessary to resort to numerical integration of equation (4).

Using the trapezoidal rule for integration, we define the following scheme:

$$\theta_{n+1} - \theta_n = \frac{h}{2}\left(f(\theta_n) + f(\theta_{n+1})\right) \tag{9}$$

with $$h = \frac{t - t_0}{N} \tag{10}$$

Since this scheme is implicit, and unconditionally stable. The following formula is used as a predictor-corrector

$$\theta_{n+1} = \theta_n + h f(\theta_n) \tag{11}$$

The function $f(\theta_n)$ is given by:

$$F(\theta_n) = \frac{C_w}{2r \sin\theta_n} \exp\left(\frac{\alpha\sigma\sqrt{1 - \cos(\theta_n)}\sqrt{2\Pi r}}{RT}\right) \tag{13}$$

Since Python is not a language adapted for scientific calculation, this task is carried out by a Fortran program called by the script.

3.6 Results

The finite element and stress corrosion models described above were used to estimate the long term strengths of two different models, namely:

i. 10 by 10 fibres and 50 longitudinal elements (Δz = 20 μm) which corresponds to an overall length of 1 mm;
ii. 15 by 15 fibres and 50 longitudinal elements (Δz = 20 μm) which corresponds to an overall length of 1 mm;

The input data used for the example is shown in Table 2. A normal probability distribution for flaw size with a mean 1.7^{o} and a variance of $.3^{o}$ was considered for illustration. For each simulation run, the flaws in each fibre element were selected randomly by sampling from the adopted flaw size distribution. Five (5) stress levels were considered in total: 300, 450, 600, 900 and 1200 MPa. Thirty (30) runs or simulations were carried out for each stress level.

Figure 14 shows the obtained results compared to with the previous shear lag results (Khennane and Melchers, 2003), the experimental results on S-glass fibres compiled by Phoenix (2000), as well as the experimental results on a unidirectional composite (UD), a chopped strand mat (CSM) and a woven roving/ chopped strand mat (WR/CSM) compiled by Clarke (1996). Interestingly, the finite element simulations are very close to the experimental results compiled by Carter on composite materials. Most importantly, it appears that the decrease in strength of the composite (fibre plus matrix) is less pronounced than that of fibres alone as shown by the slope of the curves. Without doubt, this is due to the matrix carrying some stress and reducing stress concentration on the fibres. This is well reproduced by the finite element model. It also appears that matrix cracking has no effect on the life of the sample when subject to stress corrosion in a saturated environment. This not surprising, since, as demonstrated previously, the matrix only takes a very small amount of the total stress. However, in practice where moisture profiles are common place, this is certainly not the case as matrix cracking would allow fore more environment ingress into the composite therefore thus causing more deleterious effects. This current area is currently under investigation.

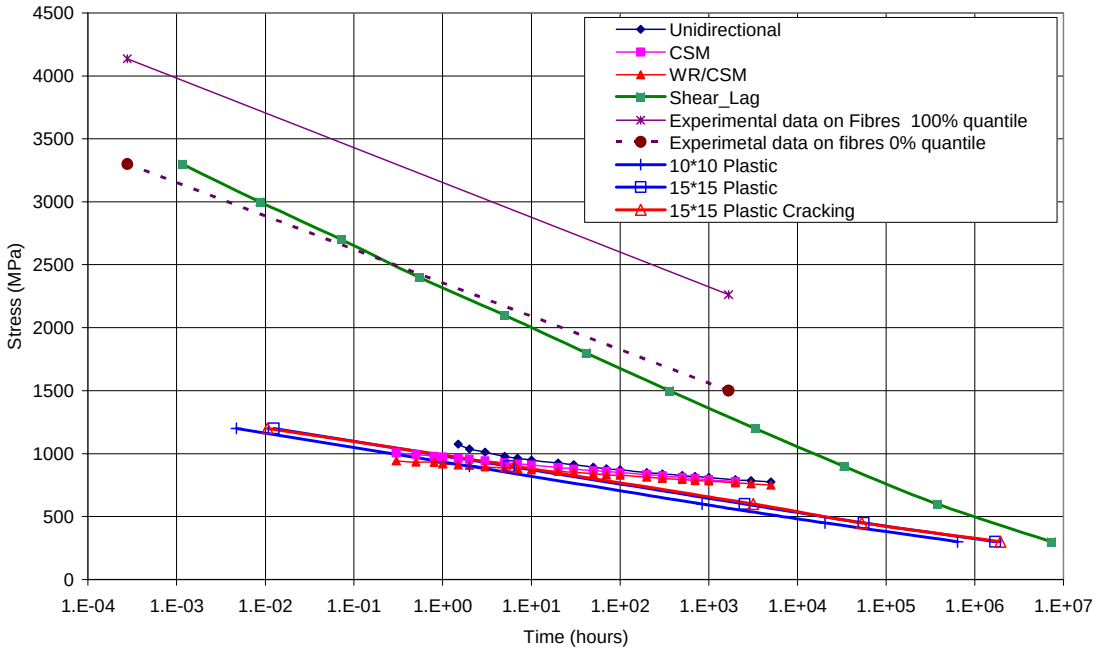

Figure 14: FEA predictions compared to shear lag and experimental data for both composites and fibres

More interestingly are the predictions concerning the instantaneous strengths. It can also be clearly seen that the corrosion model used herewith with the finite element model predicts an instantaneous strength of about 1200 MPa, which is consistent with the previously estimated strength using the Weibull statistic model Figure 4. To further enhance the validity of the model, the predictions obtained with exactly the same stress corrosion model using shear lag (Khennane and Melchers, 2003), where the matrix transfers only shear stresses, are added. It can be seen that the ultimate strength predicted by simulation is about 3.3 GPa. This is about correct when compared to known strength of E-glass unidirectional composite, which lies between 2.5 and 3.5 GPa

Unlike the previous simulations concerning the instantaneous strength, where virtually no size effect was displayed because of the relative small number of fibres used, the long term strength simulations displayed some size effect as can be clearly seen on Figure 15 where only the finite element predictions are represented.

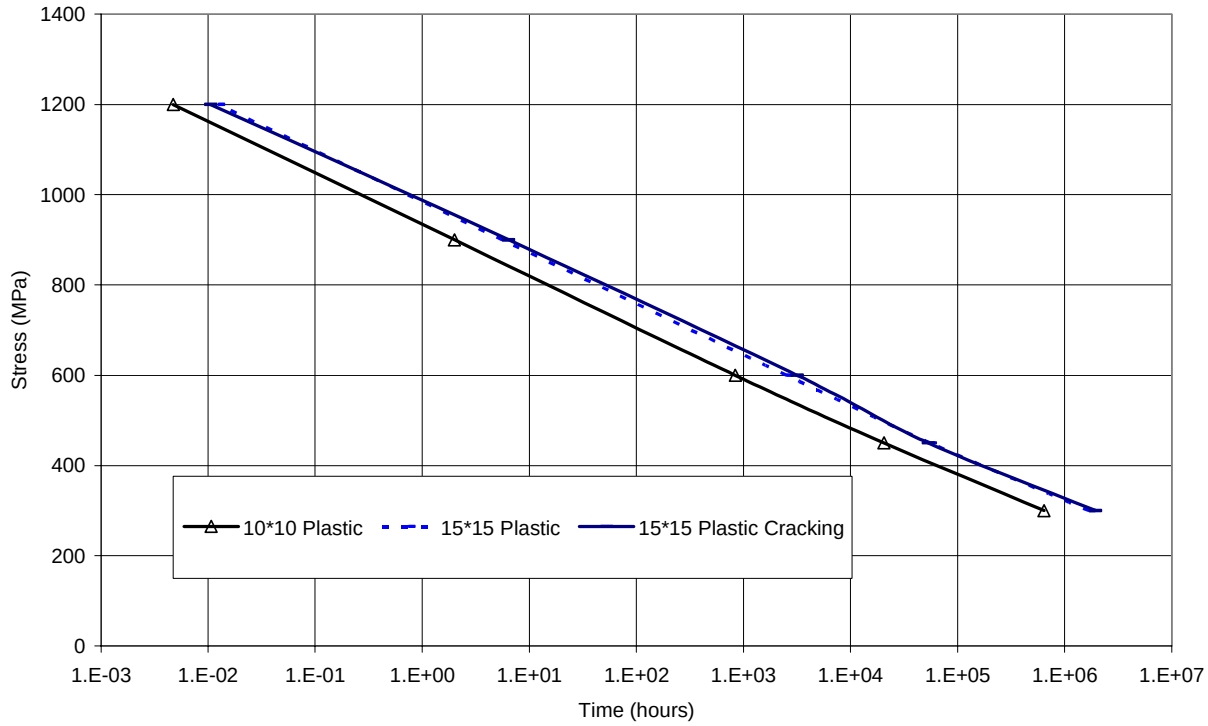

Figure 15: Size effect in FEA predictions

It can be seen that for a given stress level the model using 10x10 fibres predicts a shorter life than the one using 15x15 fibres, and this is valid for all stress levels. Furthermore, it appears that the difference is constant all the way when plotted in a logarithmic scale as shown here. This difference cannot be attributed to statistical randomness, as thirty simulations where carried out for each stress level. An explanation to this phenomenon is not available at present. This requires further investigation through simulating larger models. It may also be worthwhile to investigate this phenomenon experimentally. It is only then that a plausible explanation could be given.

Figures 16 to 20 show the percentage of fibre breaks with time for the different stress levels. In all the figures, an incubation period is evident. At low stress, about one third of the fibres fail sequentially before a quick succession of events causes the sudden failure of the composite. This is consistent with experimental observations reported by Swit (2000). As the level of stress increases, the incubation period becomes shorter. At 1200 MPa, which

corresponds to the short term uniaxial strength, ultimate failure happens after only 12 % of fibre breaks.

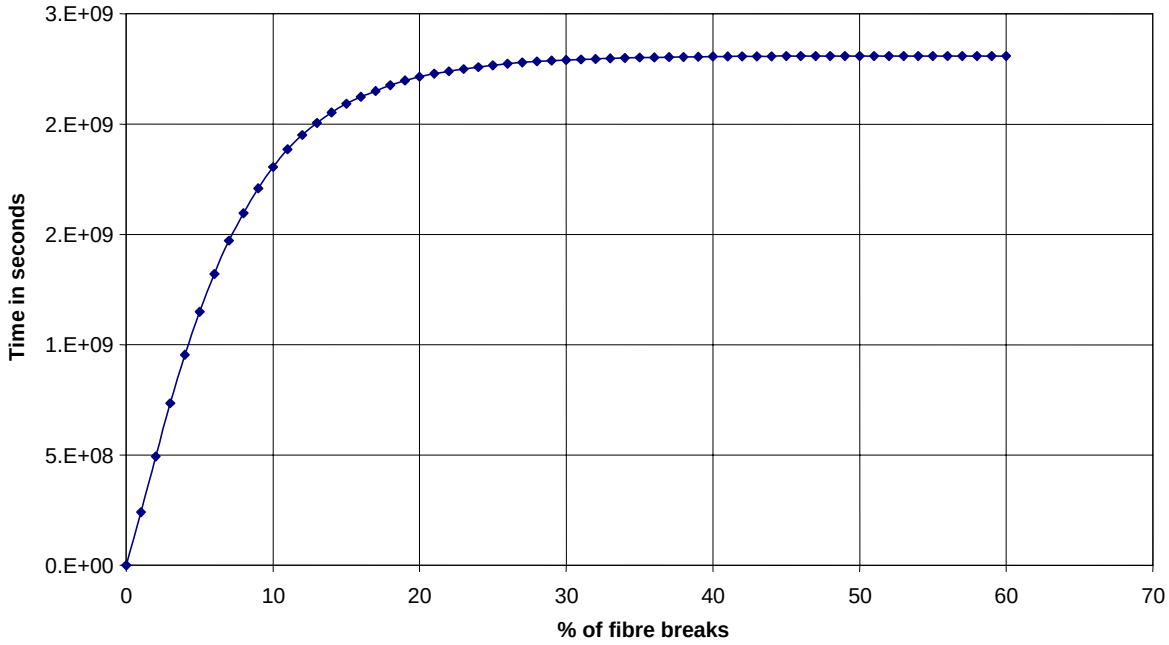

Figure 16: Fibre break events versus time at 300 MPa

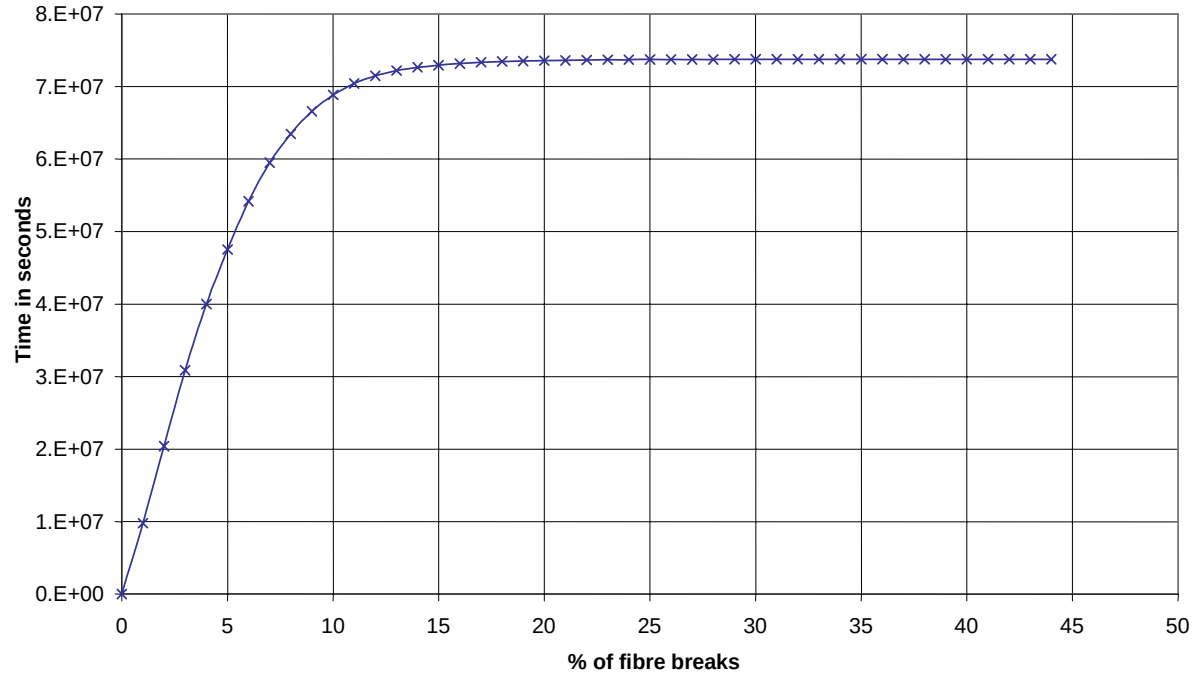

Figure 17: Fibre break events versus time at 300 MPa

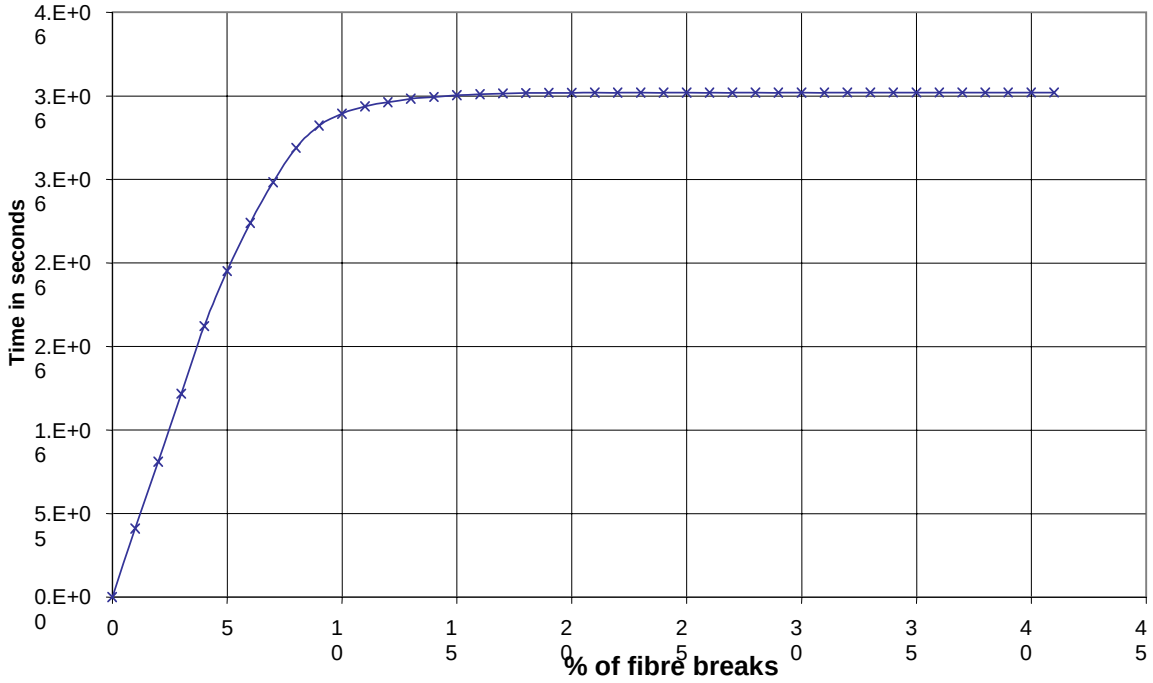

Figure 18: Fibre break events versus time at 600 MPa

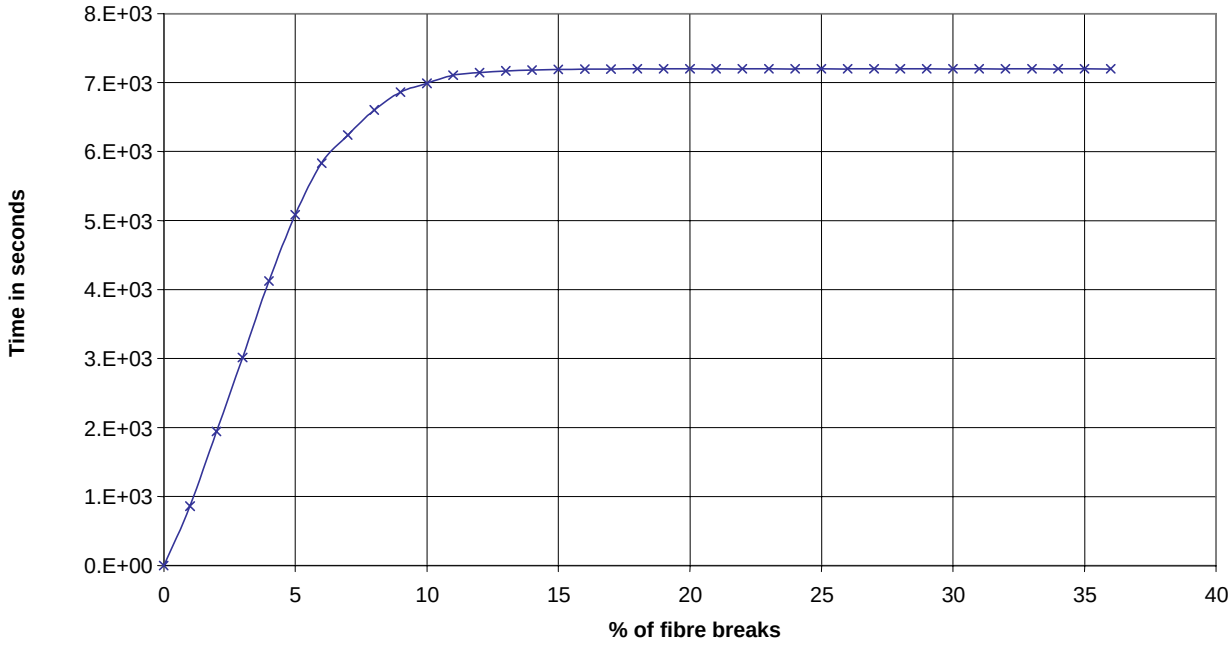

Figure 19: Fibre break events versus time at 900 MPa

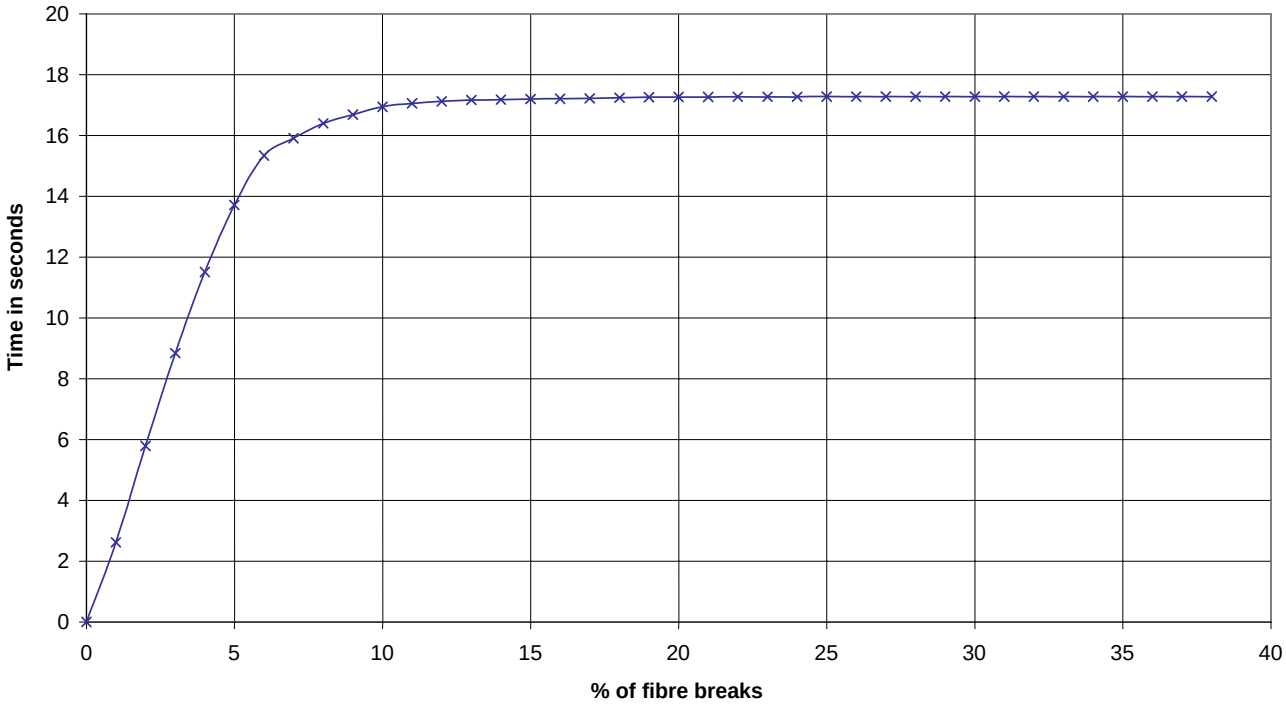

Figure 20: Fibre break events versus time at 1200 MPa

3.7 Discussion

A methodology for the prediction of the long term strength of unidirectional GFRP in tension is presented. The model is based both on a well-established knowledge on the chemical behaviour of glass and in particular that of glass flaws and more recent models of stress corrosion. These were combined with fracture mechanics, the finite element method, and a probability model for flaw size to develop a model for the description of the behaviour of GFRP composite subject to stress corrosion in three dimensions. The stress corrosion cracking of GFRP was found to have an incubation period in which about a third of the fibres break. Thereafter, the stress concentration reaches such a high level that unstable crack growth occurs. This corroborates the generally recognised catastrophic failure of static fatigue (Swit, 2000). The model also revealed that matrix cracking has no effect on the life of the sample when subject to stress corrosion in a saturated environment. However, in practice where moisture profiles are present this may not be the case as matrix cracking would certainly allow for more moisture diffusion into the composite therefore causing more deleterious effects. This current area is currently under investigation. The observations of the instantaneous strength predicted with the stress corrosion model showed complete consistency with that predicted using the Weibull probability distribution for fibre strength detailed in the first part of the paper. Unlike the simulations concerning the instantaneous strength, where virtually no size effect was displayed because of the relative small number of fibres used, the long term strength simulations displayed some size effect.

4 CONCLUSIONS

A finite element model based on the mesoscopic approach has been proposed for the simulation of the short and long terms micro-mechanical strength of glass fibre reinforced polymers. Bearing in mind that the performance of a composite material is governed by its internal structure, the approach proposed models the fibres and the matrix material as separate entities each with their own discretisation and material behaviour. The complete three-dimensional finite element modelling solution to the governing equations (equilibrium, compatibility, and constitutive behaviour) was presented in the first part of the paper. The essence of the model is a division of the composite system into a binary system comprising "fibre elements", which represent axial tow properties only, and matrix "effective medium" elements, which account for other mechanical properties such as shear and transverse stiffness and Poisson's effect. Such a representation allows taking advantage of the power of the finite element technique, and, at the same time, alleviates some of its computational impact. It is an approach also used for finite element modelling of other combinations of materials, such as reinforced concrete. This means that there is already some degree of successful experience and expertise available with this approach. It means that there can be a reasonable level of confidence in the modelling approach.

Another advantage of the use of finite element modelling is the ability to take into account of matrix cracking and long term effects. In the second part of the paper, a methodology for life prediction of unidirectional GFRP in tension is presented. The model is based both on a well-established knowledge on the chemical behaviour of glass and in particular that of glass flaws and more recent models of stress corrosion. The stress corrosion cracking of GFRP was found to have an incubation period in which about a third of the fibres break. Thereafter, the stress concentration reaches such a high level that unstable crack growth occurs. This corroborates the generally recognised catastrophic failure of static fatigue.

Finally, the results of the present study, although limited to rather idealised situations, are very encouraging. They suggest that, with only modest assumptions about material properties, it is possible to obtain mechanisms of GFRP breakdown, which corresponds to experimental behaviour, at least for the known test results. As far as can be ascertained, this has not previously been done and reported in the literature. In addition, this present study opens up a number of opportunities. In principle it is now possible to study the micro-mechanical failure of fibre reinforced composites under different states of stress such as torsion and bending.

5 REFERENCES

1. Bartenev, G.M. (1969). "Constitution and strength of glass fibers". Inter. J. of Fract. Mech., 5, 179-186
2. Byars E.A., Waldron, P. Dejke V. and Sotiris, D. (2001). Durability of FRP in concrete current specifications and a new approach." CICE 2001 International Conference on FRP Composites in Civil Engineering 12-14 December 2001, Hong Kong, pp:1497-1507
3. CERF (2000-a): "The PAIR implementation Plan - A Partnership for the Advancement of Infrastructure and its Renewal through Innovative Products And Practices, http://www.cerf.org/PDFS/pairimp.pdf
4. CERF (2000-b): "What a High- Performance Materials and Systems Program Offers" http://www.cerf.org/conmat/inside/reprtpdf/ch5.pdf
5. CERF(1997): "Accelerated Aging Techniques to Predict the Durability of FRP composites". http://www.cerf.org/research/clusters/3-2.htm
6. Chang F. K. and Lessard L. B. (1991), Damage Tolerance of laminated Composites Containing an Open Hole and Subjected to Compressive Loadings: Part I – Analysis. Journal of Composite Materials, Vol. 25, pp: 2-43
7. Charles, R. J. (1958a). "Static fatigue of glass, I". J. of Appld Physics, 29(11),1549-1553
8. Charles, R.J. (1958b). "Static fatigue of glass, II". J. of Appld Physics, 29(11),1554-1560
9. Chin, J.W. (1996): "Materials Aspects of Fibre-Reinforced Polymer Composites in Infrastructure". Building and Fire Research Laboratory, National Institute of standards and Technology. Gaithersburg, MD 20899, USA.
10. Clarke, J. L. (1996 Ed) Structural Design of Polymer Composites- EUROCOMP Design Code and Handbook. E & FN Spon London.
11. Cox, B.N., Carter, W.C. and Fleck N.A. (1994) A binary model of textile composites - I. Formulation. Acta Metall. Mater. 42 (10): 3463-3479
12. Fiedler B, Hojo M, Ochiai S, Schulte K and Ando C. Failure Behaviour of an epoxy matrix under different kinds of static loading. Composites Science and Technology 61 (2001) 1615-1624
13. Hedgepeth, J.M., Van Dyke. (1967). "Local Stress Concentrations in Imperfect Filamentary Composite Materials". J. of Comp. Mater., 1, 294-309
14. Hibbitt, Karlsson & Sorensen, Inc.(2003).Abaqus Version 6.3. Pawtucket, R.I. 02860, USA.
15. Hogg, P.J., and Hull, D. (1982). "Micromechanics of crack growth in composite materials under corrosive environments". Metal Science, 17, 441-450
16. Khennane, A. and Melchers, R.E. (2000).: "Fiber reinforced Polymers for Infrastructure Applications Durability and Life Predictions – A review". CRC-ACS report No TM 00042, 2000
17. Khennane, A. and Melchers, R. E. (2003) "Durability of Glass Polymer Composites Subject to Stress Corrosion". ASCE Journal of Composites for Construction. Vol. 7 (2), pp:109-117
18. Landis, CM , Beyerlein IJ, and McMeeking RM. Micromechanical simulation of the failure of fibre reinforced composites. J Mech Phys Solids 2000; 48: 621-48
19. Lhymn, C. and Schultz, J.M. (1983). Chemically assisted fracture of thermoplastic PET reinforced with short E-glass fibre. J. of Mater. Sci., 18, 2923-2938.
20. Liao, K., Schultheisz, C.R., Hunston, D.L. and Brinson,L.C.(1998): "Long term Durability of Fiber Reinforced Polymer Matrix Composite Materials for Infrastructure Applications: A Review". Journal of Advanced Materials
21. Lutz M & Ascher D. (1999). Learning Python.O'Reilly Sebastopol, Ca. USA

22. Lyons, K.B. and Phillips, M.G. (1981). “Creep rupture and damage mechanisms in glass reinforced plastics”. Composites, 12(4), 265-271
23. McBagonluri, F. (1998): “Simulation of fatigue performance and creep rupture of glass-reinforced polymeric composites for infrastructure applications”. MS Thesis, Virginia Polytechnic Institute and State University.
24. Mould, R.E.(1960). “Strength and static fatigue of abraded glass under controlled ambient conditions: III, Aging of fresh abrasions”. J. of the Amer. Ceram Soc., 43, 160-167
25. Nedele, MR and Wisnom, MR. 1994. Three dimensional finite element analysis of the stress concentration at a single fibre break. Comp. Sci. Technol. 51, 517-524
26. Okabe, T., Takeda, N., Kamoshida, Y., Shimizu, M. and Curtin, W.A . (2001). A 3D shear-lag model considering micro-damage and statistical strength prediction of unidirectional fibre-reinforced composites. Composites Science and technology. 61: 1773-1787
27. Okabe T. and Takeda N. (2002). Size effect on tensile strength of unidirectional CFRP composites-experiment and simulation Composites Science and Technologie, 62 pp:2053-206410
28. Phillips, M.G. (1983). “Prediction of long term stress-rupture life for glass fibre reinforced polyester composites in air and aqueous environments”. Composites, 14(3), 270-275
29. Phoenix, S.L.(2000). “Modelling the statistical lifetime of glass fiber/polymer matrix composites in tension”. Comp. Struct., 48, 19-29
30. Reedy, E.D. Jr.(1984). “Fiber stresses in a cracked monolayer: Comparison of shear lag and 3-D finite element Predictions”. J. of Comp. Mater., 18, 595-607
31. Roberts, R.C. (1978). “Design strain and failure mechanisms of GRP in a chemical environment”. Reinforced Plastics Congress, British Plastics Federation, 145-151
32. Sastry, A.M. and Phoenix S.L. (1993). “Load redistribution near non-aligned fibre breaks in a two-dimensional unidirectional composite using break-influence superposition”. J. of Mater. Sci. Lters 1993, 12, 1596-1599.
33. Schmitz, G.K. and Metcalfe, A.G. (1965). “Characterisation of flaws on glass fibres”. Proceedings of the 20th Anniversary Technical Conference. The Society of the Plastics Industry, INC. p.1-14
34. Schmitz, G.K., and Metcalfe, A.G. (1966). “Stress corrosion of E-glass fibres”. I&EC Products Res. Dev. Indust. & Engrg Chem., 5(1),1-8
35. Schutte, C.L. (1994). “Environmental durability of glass-fiber composites”. Mater. Sc. and Engrg, R13(7), 265-324
36. Sekine, H., and Beaumont, P.W.R. (1998). “A physically Based Micromechanical Theory and Diagrams of Macroscopic Stress-Corrosion Cracking in Aligned Continuous Glass-Fibre-Reinforced Polymer Laminates”. Composites Sc. and Tech., 58,1659-1665.
37. Schutte, C.L.(1994): ”Environmental durability of glass fiber composites”. Materials Science and Engineering, R13, No 7, pp 264-324.
38. Swit, G.(2000). “Durability of stressed E-glass fibre in alkaline medium”. In Recent Developments in Durability Analysis of Composite Systems. Cardon, Fukuda, Reifsneider and Verchery Editions, Balkema, Rotterdam, 473-476
39. van Rossum G. (2001). Python Tutorial. Fred L. Drake, Jr., editor, PythonLabs, E-mail: pythondocs@python.org, http://www.python.org/doc/current/tut/tut.html
40. Wiederhorn, S.M., and Bolz, L.H. (1970). “Stress corrosion and static fatigue of glass”. J. of the Amer. Ceram. Society, 53(10), 543-548
41. Zhou, S. J. and Curtin,W.A. (1995). “Failure of fibre composites: A lattice Green function model”. Acta. Metall. Mater, 43(8),3093-3104

Acknowledgement

The first author gratefully acknowledges the financial support provided by The University of Southern Queensland Early Career Researcher Program (ECRP).